Chapter 5

Large scale shell model calculations for odd-odd $^{58-62}$Mn isotopes

5.1 Introduction

The region of the neutron-rich *fp* shell nuclei between the magic numbers N=28 and N=50 has been at the focus of recent experimental and theoretical studies. The actual mechanism which causes the changes in nuclear structure as neutron number increases in a nuclear system is still an open question. Neutron rich *fp* shell nuclei are also of special interest in astrophysics such as the electron capture rate in supernovae explosion. However the experimental data on neutron rich *fp* shell nuclei is limited to those that can be populated by different experimental techniques. Recently energy levels of odd-odd $^{58-62}$Mn isotopes have been reported in the literature. Appelbe *et al.* [App00] have populated the high spin states of ^{58}Mn by bombarding 40 MeV ^{13}C beam upon an enriched ^{48}Ca target. The level scheme of ^{59}Mn was reported by Liddick *et al.* [Lid05] following β-decay of ^{59}Cr. The excited states of ^{60}Mn were populated following the β-decay of ^{60}Cr [Lid06]. Gaudefroy *et al.* [Gau05] have studied β decay of ^{62}Cr to ^{62}Mn, but the location and ordering of the proposed 1^+ and 4^+ states in ^{62}Mn are very puzzling. Valiente-Dobón *et al.* [Dob08] studied neutron-rich Mn isotopes from A=59-63, through multi-nucleon transfer reaction by bombarding a ^{238}U target with 460 MeV ^{70}Zn beam. The identification of γ-rays belonging to each nucleus was carried out with high precision by coupling the clover detector of Euroball (CLARA) to PRISMA magnetic spectrometer. This experiment has provided data on the level structure of neutron rich Mn isotopes from A=59 to 63. Crawford *et al.* [Cra09] have studied the β decay of ^{61}Cr for non-yrast excited states in the daughter nucleus ^{61}Mn.

In the present work we have performed large scale shell model calculations on neutron rich $^{58-62}$Mn isotopes in two different model spaces. The aim of the present work is to test (i) the recent experimental data on neutron rich Mn isotopes (ii) suitability of valence space and the available (iii) effective interactions for *fp* shell nuclei in the frame work of large scale shell model calculations. Odd-odd $^{58-62}$Mn isotopes are associated with two shell closures: Z = 20, N = 20 and Z = 20, N = 28. In view of this we have performed two sets of calculations. In the first set valence space is of full *fp* shell consisting of $0f_{7/2}$, $1p_{3/2}$, $0f_{5/2}$, $1p_{1/2}$ orbitals and treating ^{40}Ca as the inert core. Second set of calculations have been performed in valence space *fpg* taking ^{48}Ca as inert core. As the dimension of the matrices becomes very large truncation has been imposed on the number of particles that can be excited.

5.2 Details of calculation

Large scale shell model calculations have been performed for neutron rich even Mn isotopes with A=58, 60, 62 in *fp* and *fpg* valence spaces. For *fp* valence space the GXPF1A and KB3G interactions have been used. The configuration space is taken as full *fp* shell which is made up of all Pauli allowed combinations of valence particles in the $0f_{7/2}$, $1p_{3/2}$, $0f_{5/2}$ and $1p_{1/2}$ orbitals for both protons and neutrons. No restriction has been put on the number of particles which can be excited to higher levels. The *fpg* model space comprises of the $0f_{7/2}$, $1p_{3/2}$, $0f_{5/2}$, $1p_{1/2}$ active proton orbitals and $0f_{7/2}$, $1p_{3/2}$, $0f_{5/2}$, $1p_{1/2}$, $0g_{9/2}$ neutron orbitals with eight $f_{7/2}$ frozen neutrons. In *fpg* we used truncation by allowing up to a total of six particle excitations from the $f_{7/2}$ orbital to the upper *fp* orbitals for protons and from the upper neutron *fp* orbitals to the $g_{9/2}$ orbital which is shown in Fig. 5.1. The single particle energies for these interactions are shown in Table 5.1.

Table 5.1: Single particle energies used in GXPF1A, KB3G and fpg interactions in MeV.

State	GXPF1A	KB3G	fpg
$f_{7/2}$	-8.6240	-8.6000	0.000
$p_{3/2}$	-5.6793	-6.6000	2.000
$p_{1/2}$	-4.1370	-4.6000	4.000
$f_{5/2}$	-1.3829	-2.1000	6.500
$g_{9/2}$	-	-	9.000

The GXPF1A interaction is obtained from a fit to the experimental data of un-

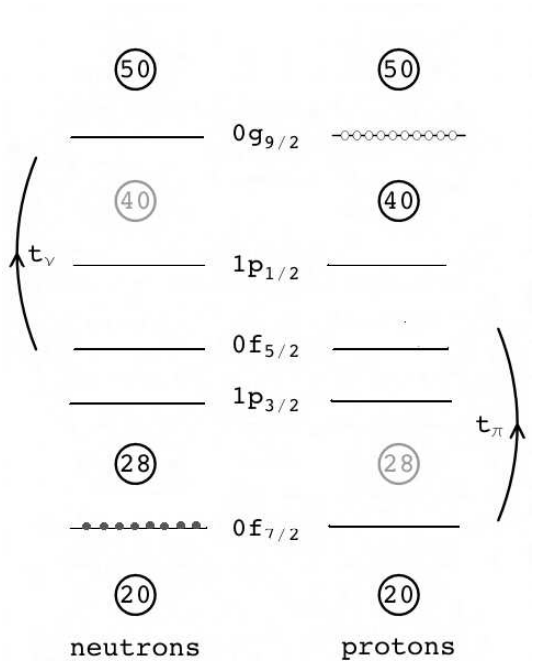

Figure 5.1: The truncation procedure used for *fpg* shell in $^{58-62}$Mn isotopes.

stable nuclei in the *fp* shell. Honma *et al.* [Hon04a] initially derived an effective interaction, GXPF1, starting from Bonn-C potential by modifying 70 well determined combinations of 4 single particle energies and 195 two body matrix elements by iterative fitting calculations to about 699 experimental energy data out of 87 stable nuclei. These authors have tested the GXPF1 interaction for the shell model calculations in the full *fp* shell extensively [Hon04a] from various viewpoints such as binding energies, electromagnetic moments, transitions and excitation spectra in the wide range of *fp* shell nuclei. They observed that the deviation of the shell model prediction from available experimental data appeared to be sizable in binding energies of N $\geq$ 35 nuclei and in magnetic moments of Z $\geq$ 32 even-even nuclei. For the unstable nuclei, whereas the experimental data on Ca and Cr isotopes were well explained with GXPF1A, the experimental value of the first excited 2^+ state of ^{56}Ti was lower than the predicted value by 0.4 MeV requiring modification of the interaction. The interaction was modified by these authors by changing 5 two body matrix elements in the *fp* shell: 3 pairing interaction matrix elements were made slightly weaker and two quadrupole-quadrupole matrix elements were made slightly stronger [Hon04b]. The modified interaction, referred to as GXPF1A, gave improved description simultaneously for all these three isotopic chains and is reliable for use in shell model calculations to explain the data on unstable nuclei. The KB3G

interaction is extracted from KB3 interaction by introducing mass dependence and refining its original monopole changes in order to treat properly the $N = Z$=28 shell closer and its surroundings [Pov01].

For the *fpg* valence space, an effective interaction was reported in Ref. [Sor02]. This interaction was built using *fp* two-body matrix elements (TBME) from Ref. [Pov01] and $1p_{3/2}$, $0f_{5/2}$, $1p_{1/2}$, $0g_{9/2}$ TBME from Ref. [Now96]. For the common active orbitals in these subspaces, matrix elements were taken from Ref. [Now96]. As the latter interaction was defined for a ^{56}Ni core, a scaling factor of $A^{-1/3}$ amplitude was applied to take into account the change of radius between the ^{40}Ca and ^{56}Ni cores. As protons are added in the $f_{7/2}$ shell, the excitation energy of the $9/2^+$ state gets decreased due to the attractive interaction $\pi f_{7/2}\nu g_{9/2}$. The remaining matrix elements were taken from $f_{7/2}g_{9/2}$ TBME from Ref. [Kah69].

The calculations have been performed at the SGI-cluster computer at GANIL with the code `ANTOINE` [Cau89] [Cau99]. In this code the problem of giant matrices is solved by splitting the valence space into two parts, one for proton and another for the neutron. The states of the basis are written as the product of two Slater determinants (SD), one for protons and another for neutrons: $\mid I\rangle = \mid i, \alpha\rangle$ (Here capital letter refers to full space and lower case letters refer to subspaces of proton and neutron). The Slater determinants i and α can be classified by their M values, M_1 and M_2. The total M being fixed, the SD of the two subspaces will be associated only if $M_1 + M_2 = M$.

5.3 Results and discussions

In Table 5.2 all the experimental and theoretical low-lying states up to 2 MeV for ^{58}Mn are listed. The results of earlier calcultions [Lid06] with GXPF1 for comparison are also shown. In Fig. 5.2 the calculated energy levels obtained with three different interactions together with the experimental data are shown. GXPF1A and KB3G interactions predict the ground state spin as 4^+ and 1^+ state lies at 41 KeV and 11 KeV above the ground state respectively. The *fpg* interaction gives the correct ground state spin 1^+ as also obtained experimentally. The first 4^+ excited state is predicted at about 26 KeV against the experimental value of 71 KeV. It is observed that in going from GXPF1 to GXPF1A and then to KB3G the predicted energy difference between the first excited 1^+ state and the 4^+ ground state decreses from 72 to 41 and then to 11 KeV. Finally when the $g_{9/2}$ orbital is included in the

valence space, the 1^+ state comes below 4^+ state as observed experimentally. This shows the importance of $g_{9/2}$ orbital in the valence space. The experimental data predicts 5^+ level at 448 KeV and 2^+ level at 1325 KeV. There are six 1^+ states

Table 5.2: Experimental and theoretical low-lying states (up to 2 MeV) of ^{58}Mn. Energies are in MeV. The results of GXPF1 interaction are taken from Ref. [Lid06].

J^π	Exp.	J^π	GXPF1	J^π	GXPF1A	J^π	KB3G	J^π	fpg
1^+	0.000	4^+	0.000	4^+	0.000	4^+	0.000	1^+	0.000
(4^+)	0.071	1^+	0.072	1^+	0.041	1^+	0.011	4^+	0.026
-	0.160	2^+	0.145	2^+	0.104	2^+	0.145	2^+	0.185
1^+	0.255	3^+	0.181	3^+	0.142	3^+	0.295	2^+	0.446
1^+	0.361	2^+	0.199	2^+	0.168	2^+	0.379	3^+	0.448
(5^+)	0.448	5^+	0.345	5^+	0.386	5^+	0.471	5^+	0.616
-	0.550	3^+	0.473	3^+	0.488	3^+	0.602	3^+	0.733
1^+	0.700	5^+	0.527	4^+	0.509	4^+	0.740	3^+	0.921
-	0.755	4^+	0.545	5^+	0.539	1^+	0.747	4^+	0.947
1^+	0.850	1^+	0.818	1^+	0.836	5^+	0.819	2^+	0.950
1^+	0.925	0^+	1.672	6^+	1.138	6^+	1.299	4^+	1.023
1^+	1.125	-	-	6^+	1.258	6^+	1.394	1^+	1.192
2^+	1.325	-	-	7^+	1.760	7^+	1.837	5^+	1.261
-	-	-	-	0^+	1.762	0^+	1.886	1^+	1.423
-	-	-	-	-	-	-	-	6^+	1.439
-	-	-	-	-	-	-	-	5^+	1.570
-	-	-	-	-	-	-	-	0^+	1.726

other than ground state and three levels with unassigned spin. In our calculation a 5^+ level is predicted at 386 KeV for GXPF1A, 471 KeV for KB3G and 616 KeV for *fpg*. The first predicted 2^+ level lies around 145 KeV and may correspond to observed experimental value of 160 KeV with unassigned spin. The second 2^+ level is predicted at 168 KeV for GXPF1A, 379 KeV for KB3G and 446 KeV for *fpg*. The number of predicted 1^+ levels below 2 MeV is two for GXPF1A, two for KB3G and three for *fpg* interaction. The most dominat wave functions for the 1^+ and 4^+ states of ^{58}Mn for different interactions are shown in Table 5.5.

In Table 5.3 all the experimental and theoretical low-lying states up to 1.6 MeV for ^{60}Mn are listed. In Fig. 5.3 we have shown the comparison of experimental values with those predicted for three different interactions. The ground state spins $J^\pi = 1^+$ is correctly reproduced by GXPF1A and KB3G interaction. The Calculated 4^+ state is at 228 KeV for GXPF1A and at 223 KeV for KB3G compared to the experimental value of 271 KeV. Two states with spin 2^+ and 3^+ have been predicted to lie between 1^+ and 4^+ state for GXPF1A. For KB3G these states lie higher than 2^+. It is observed that *fpg* interaction does not predict correct ground state spin. The composition of ground state wave function is given in Table 5.6.

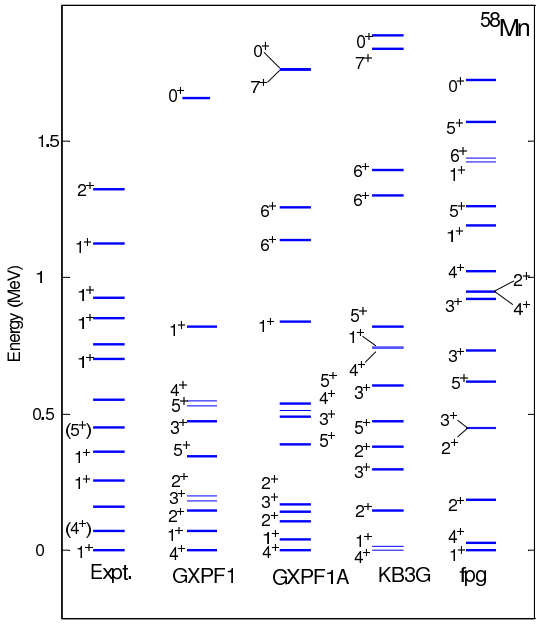

Figure 5.2: Comparison of the large-scale shell model calculations of ^{58}Mn using various effective interaction with the experimental values taken from Ref. [Lid06] [NNDC]. The results of GXPF1 interaction taken from Ref. [Lid06].

In Table 5.4 we list experimental ground state and all theoretical low-lying states up to 1 MeV for ^{62}Mn isotope. In Fig. 5.4 we have shown the comparison of experimental values with those predicted for three different interactions. Experimentally for ^{62}Mn there is an uncertainty in assigning the ground state spin to be 1^+, 3^+ or 4^+. All the calculated results show 2^+ level as the ground state showing the inadequacy of the used valence space.

The composition of ground state and first excited state wave functions of ^{62}Mn are given in Table 5.7. In the ground states of ^{58}Mn and ^{60}Mn and in the first excited state of ^{58}Mn the probability of occupancy of $0g_{9/2}$ orbital is very small. However for the first excited level of ^{60}Mn and the first two levels of ^{62}Mn the occupancy $0g_{9/2}$ level is gets increased.

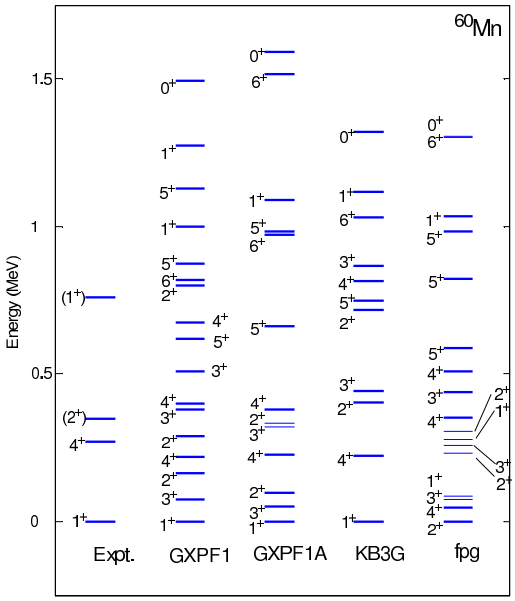

Figure 5.3: Comparison of the large-scale shell model calculations of ^{60}Mn using various effective interaction with the experimental values taken from Ref. [Lid06] and NNDC. The results of GXPF1 interaction are taken from Ref. [Lid06].

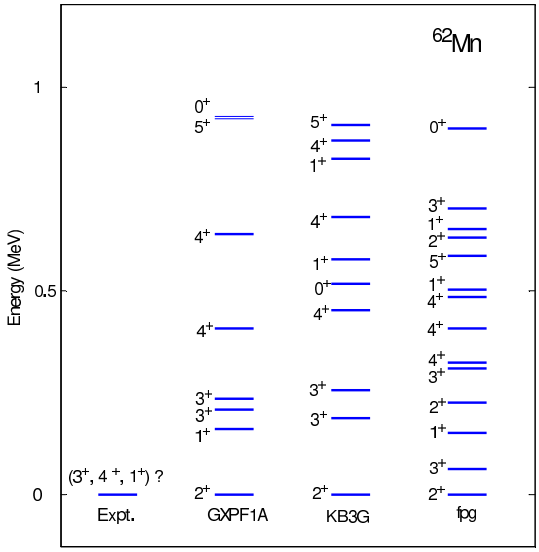

Figure 5.4: Comparison of the large-scale shell model calculations of ^{62}Mn using various effective interaction with the experimental values taken from Ref [Gau05] and NNDC.

Table 5.3: Experimental and theoretical low-lying states (up to 1.6 MeV) of ^{60}Mn. Energies are in MeV. The results of GXPF1 interaction taken from Ref. [Lid06] [NNDC].

J^π	Exp.	J^π	GXPF1	J^π	GXPF1A	J^π	KB3G	J^π	fpg
1^+	0.000	1^+	0.000	1^+	0.000	1^+	0.000	2^+	0.000
4^+	0.271	3^+	0.072	3^+	0.050	4^+	0.223	4^+	0.048
(2^+)	0.349	2^+	0.164	2^+	0.097	2^+	0.402	3^+	0.072
(1^+)	0.759	4^+	0.218	4^+	0.228	3^+	0.444	1^+	0.087
-	-	2^+	0.291	3^+	0.319	2^+	0.716	2^+	0.229
-	-	3^+	0.381	5^+	0.332	5^+	0.749	3^+	0.259
-	-	4^+	0.400	4^+	0.380	4^+	0.815	1^+	0.277
-	-	3^+	0.509	5^+	0.663	3^+	0.866	2^+	0.303
-	-	5^+	0.618	6^+	0.970	6^+	1.032	4^+	0.353
-	-	4^+	0.672	5^+	0.985	1^+	1.118	3^+	0.438
-	-	2^+	0.800	1^+	1.088	0^+	1.322	4^+	0.510
-	-	6^+	0.818	6^+	1.518	-	-	5^+	0.589
-	-	5^+	0.873	0^+	1.591	-	-	5^+	0.823
-	-	1^+	1.000	-	-	-	-	5^+	0.983
-	-	5^+	1.127	-	-	-	-	1^+	1.033
-	-	1^+	1.273	-	-	-	-	6^+	1.301
-	-	0^+	1.491	-	-	-	-	0^+	1.305

Table 5.4: Experimental and theoretical low-lying states (up to 1 MeV) of ^{62}Mn. Energies are in MeV.

J^π	Exp.	J^π	GXPF1A	J^π	KB3G	J^π	fpg
$(3^+,4^+,1^+)$?	0.000	2^+	0.000	2^+	0.000	2^+	0.000
-	-	1^+	0.161	3^+	0.188	3^+	0.063
-	-	3^+	0.208	3^+	0.258	1^+	0.154
-	-	3^+	0.236	4^+	0.454	2^+	0.227
-	-	4^+	0.407	0^+	0.519	3^+	0.310
-	-	4^+	0.641	1^+	0.579	4^+	0.325
-	-	5^+	0.922	4^+	0.681	4^+	0.408
-	-	0^+	0.927	1^+	0.823	4^+	0.486
-	-	-	-	4^+	0.868	1^+	0.502
-	-	-	-	5^+	0.908	5^+	0.588
-	-	-	-	-	-	2^+	0.630
-	-	-	-	-	-	1^+	0.652
-	-	-	-	-	-	3^+	0.702
-	-	-	-	-	-	0^+	0.897

5.4 Conclusions

In the present work large scale shell model calculations have been performed for neutron rich odd-odd isotopes of Mn with A=58, 60, 62 in two valence spaces: full *fp* space and *fpg* space. For *fp* space calculations have been performed with recently derived GXPF1A and KB3G interactions without truncation. For *fpg* space

Table 5.5: Main configurations in the wave functions of the ground state and the first exited state for ^{58}Mn for different interactions.

Nuclei	J^π	Wave function		Probability
		Neutron	Proton	
GXPF1A	4^+_{gs}	$(0f_{7/2})^8,(1p_{3/2})^3,(0f_{5/2})^2,(1p_{1/2})^0$	$(0f_{7/2})^5$	25.9
	1^+_1	$(0f_{7/2})^8,(1p_{3/2})^3,(0f_{5/2})^2,(1p_{1/2})^0$	$(0f_{7/2})^5$	22.0
KB3G	4^+_{gs}	$(0f_{7/2})^8,(1p_{3/2})^3,(0f_{5/2})^2,(1p_{1/2})^0$	$(0f_{7/2})^5$	34.4
	1^+_1	$(0f_{7/2})^8,(1p_{3/2})^3,(0f_{5/2})^2,(1p_{1/2})^0$	$(0f_{7/2})^5$	28.1
fpg	1^+_{gs}	$(0f_{7/2})^8,(1p_{3/2})^3,(0f_{5/2})^2,(1p_{1/2})^0,(0g_{9/2})^0$	$(0f_{7/2})^5$	21.4
	4^+_1	$(0f_{7/2})^8,(1p_{3/2})^3,(0f_{5/2})^2,(1p_{1/2})^0,(0g_{9/2})^0$	$(0f_{7/2})^5$	23.9

Table 5.6: Main configurations in the wave functions of the ground state and the first exited state for ^{60}Mn for different interactions.

Nuclei	J^π	Wave function		Probability
		Neutron	Proton	
GXPF1A	1^+_{gs}	$(0f_{7/2})^8,(1p_{3/2})^4,(0f_{5/2})^3,(1p_{1/2})^0$	$(0f_{7/2})^5$	25.9
	3^+_1	$(0f_{7/2})^8,(1p_{3/2})^4,(0f_{5/2})^2,(1p_{1/2})^1$	$(0f_{7/2})^5$	22.0
KB3G	1^+_{gs}	$(0f_{7/2})^8,(1p_{3/2})^4,(0f_{5/2})^3,(1p_{1/2})^0$	$(0f_{7/2})^5$	34.4
	4^+_1	$(0f_{7/2})^8,(1p_{3/2})^4,(0f_{5/2})^3,(1p_{1/2})^0$	$(0f_{7/2})^5$	28.1
fpg	2^+_{gs}	$(0f_{7/2})^8,(1p_{3/2})^4,(0f_{5/2})^2,(1p_{1/2})^1,(0g_{9/2})^0$	$(0f_{7/2})^5$	21.4
	4^+_1	$(0f_{7/2})^8,(1p_{3/2})^3,(0f_{5/2})^2,(1p_{1/2})^0,(0g_{9/2})^2$	$(0f_{7/2})^5$	23.9

calculations have been performed with *fpg* interaction using truncation. In going from ^{58}Mn to ^{60}Mn the experimental value for the separation between first excited 4^+ state and 1^+ ground state increses from 71 KeV to 271 KeV. Even though the *fpg* interaction in the truncated space does not reproduce ground state spin for ^{60}Mn it is likely that expanding the valence space to include more orbitals from *sdg* shell and/or relaxing the truncation may predict the correct ground state spin and the $4^+ \sim 1^+$ separation. A key feature yet to be identified in the neutron rich odd-odd Mn

Table 5.7: Main configurations in the wave functions of the ground state and the first exited state for ^{62}Mn for different interactions.

Nuclei	J^π	Wave function		Probability
		Neutron	Proton	
GXPF1A	2^+_{gs}	$(0f_{7/2})^8,(1p_{3/2})^4,(0f_{5/2})^4,(1p_{1/2})^1$	$(0f_{7/2})^5$	25.9
	1^+_1	$(0f_{7/2})^8,(1p_{3/2})^4,(0f_{5/2})^3,(1p_{1/2})^2$	$(0f_{7/2})^5$	22.0
KB3G	2^+_{gs}	$(0f_{7/2})^8,(1p_{3/2})^4,(0f_{5/2})^4,(1p_{1/2})^1$	$(0f_{7/2})^5$	34.4
	3^+_1	$(0f_{7/2})^8,(1p_{3/2})^4,(0f_{5/2})^4,(1p_{1/2})^1$	$(0f_{7/2})^5$	28.1
fpg	2^+_{gs}	$(0f_{7/2})^8,(1p_{3/2})^4,(0f_{5/2})^2,(1p_{1/2})^1,(0g_{9/2})^2$	$(0f_{7/2})^5$	21.4
	3^+_1	$(0f_{7/2})^8,(1p_{3/2})^4,(0f_{5/2})^2,(1p_{1/2})^1,(0g_{9/2})^2$	$(0f_{7/2})^5$	23.9

isotopes is the location of the negative parity levels that could signify the presence of including $1g_{9/2}$ orbital. More experimental data on ^{62}Mn and higher neutron-rich Mn isotopes are needed to discuss the onset of the collectivity while approaching N =40.